ISSN: 0975-8585

Research Journal of Pharmaceutical, Biological and Chemical Sciences

Nano-Dispersed Fe_3O_4 Liquid Crystal Compound Image Enhancement using Advanced Histogram Equalization Technique.

J Sivasri[1], B T P Madhav[2], M C Rao[3], and R K N R Manepalli[1]*.

[1]Department of Physics, The Hindu College, Krishna University, Machilipatnam-521001, India
[2]LCRC-R&D, Department of ECE, K L University, Guntur-522502, India
[3]Department of Physics, Andhra Loyola College, Vijayawada-520008, India

ABSTRACT

Various methods are evolved to enhance the quality of textural image like gray scale manipulation, filtering and Histogram. Histogram equalization technique is popular technique because of its simplicity and effectiveness in image enhancement. This paper is aimed to enhance the contrast image phases of liquid crystalline p-n- nonyloxy benzoic acid (9OBA) with 1 wt % dispersed Fe_3O_4 nanoparticles, by considering global and local image information. Preservation of the input brightness of the textural image is required to avoid the generation of non-existing artefacts in the output image. This method preserves the input brightness on the output image with a significant contrast enhancement. It is used to identify the uniform regions and to detect the defects which are not clearly observed from the textures that are recorded by Polarising Microscope (POM) and Differential Scanning Calorimeter (DSC). The studies of nanodispersed p-n-nonyloxy benzoic acid exhibit nematic and smectic c phases with reduced transition temperatures as expected and the nematic thermal ranges are increased by 4 to 5 ^oC while observing through POM and DSC.

Keywords: Image processing, nanodispersed LCs, POM, DSC, Image Enhancement and Histogram.

Corresponding author

ISSN: 0975-8585

INTRODUCTION

For both human and computer vision contrast enhancement is an important area in image processing. Image enhancement is a process of making output image look better by changing the pixels intensity of input image [1]. It is widely used for medical image processing and as a pre-processing step in speech recognition, texture synthesis and many other image/video processing applications [2-5]. Confucius said, a picture is worth a thousand words [6]. Image Enhancement is simple and most appealing area among all the digital image processing techniques. The main purpose of image enhancement is to bring out detail that is hidden in an image or to increase contrast in a low contrast image. By using brightness preserving bi-histogram method [7], the contrast has been enhanced. Similarly the contrast of the image is enhanced by using block over lapped histogram equalization technique [8] and by other histogram based methods [9-14]. Rao et al. have presented the results on different oxide materials in their earlier studies [15-20]. In this paper we observed the textures of LC phases with dispersed nanoparticles obtained from POM are having less brightness. In order to increase the contrast of image of textures and to find out the defects, the histogram equalization technique is implemented.

EXPERIMENTAL

Fe_3O_4 nanoparticles and pure LC compound p-n-nonyloxybenzoic acid (9OBA) are bought from sigma Aldrich Laboratories, USA and are used as such without any further purification. For uniform dispersion, the Fe_3O_4 nano particles first dissolved in ethyl alcohol, stirred well in Ultrasonic bath about 45 minutes and later introduced in the isotropic state of mesogenic material 9OBA. After cooling the nano dispersed 9OBA is subjected to study the textural and phase transition temperatures using polarizing optical microscope with the hot stage in which the substance, (sandwiched between a glass plate and cover slip) can be placed along with the thermometer described by Gray [21]. Textural and phase transition temperatures are studied after preparation of the sample and observations are made again to understand the stability of Fe_3O_4 nanoparticles. DSC is used to obtain the transition temperatures and the enthalpy values. The image processing program was coded in MATLAB tool for computational analysis of nano doped liquid crystalline textures.

HISTOGRAM EQUALIZATION

When dealing with discrete quantities, we work with histograms and call the preceding technique histogram equalization, although in general, the histogram of the processed image will not be uniform, due to discrete nature of the variables. Let Pr (rj), j =1, 2… L, denotes the histogram associated with the intensity levels of a given image and recall that the values in a normalized histograms are approximations to the probability of occurrence of each intensity level in the image. For discrete quantities we work with summations and the equalization transformation becomes

$$S_k = T(r_k)$$

$$= \sum_{j=1}^{k} Pr(rj)$$

$$= \sum_{j=1}^{k} \frac{nj}{n}$$

For k = 1, 2… L, where is the intensity value in the output image corresponding to value r_k in the input image.

Histogram equalization is implemented by g = histeq (f, nlev)

Where ‘f’ is the input image and ‘nlev’ is the number of intensity levels specified for the output image. If nlev is equal to ‘L’ (the total number of possible levels in the input image), then histogram equalization implements the transformation function, $T(r_k)$, directly. If nlev is less than ‘L’, then histogram equalization attempts to distribute the levels so that they will approximate a flat histogram. Unlike ‘imhist’ the default

value in histogram equalization is nlev = 64. For the most part, we use the maximum possible number of levels (generally 256) for nlev because this produces a true implementation of the histogram equalization method.

RESULTS AND DISCUSSION

Figure-1 shows the collected image of 9OBA pure compound isotropic to nematic transition at 134.9 ^{o}C from digital camera connected to polarizing microscope with hot stage. Figure- 1(a) shows the image of 9OBA nematic droplets at transition temperature 134.9 ^{o}C. In terms of needed enhancement, the most important features of this image are that, it is dark and has low dynamic range. This can be observed from Figure-1(a), in which the dark nature of the image is expected because the histogram is biased toward the dark end of the gray scale. The low dynamic range is evident from the fact that the width of the histogram is narrow with respect to entire gray scale. The image in Figure-1(b) shows the converted image of NTSC to equivalent true RGB color image, where NTSC is a standard color encoding scheme. Figure- 1(c) is the histogram equalized result.

(a) (b) (c)

Figure-1: (colour online) Analysis of 9OBA pure compound (nematic droplets). Isotropic to nematic transition 134.9 ^{o}C (2272× 1704 pixels):1(a) nematic droplets at isotropic to nematic transition obtained from thermal microscopy, 1(b) true RGB colour image of original texture1 (a), 1(c) histogram equalized image with contrast enhancement

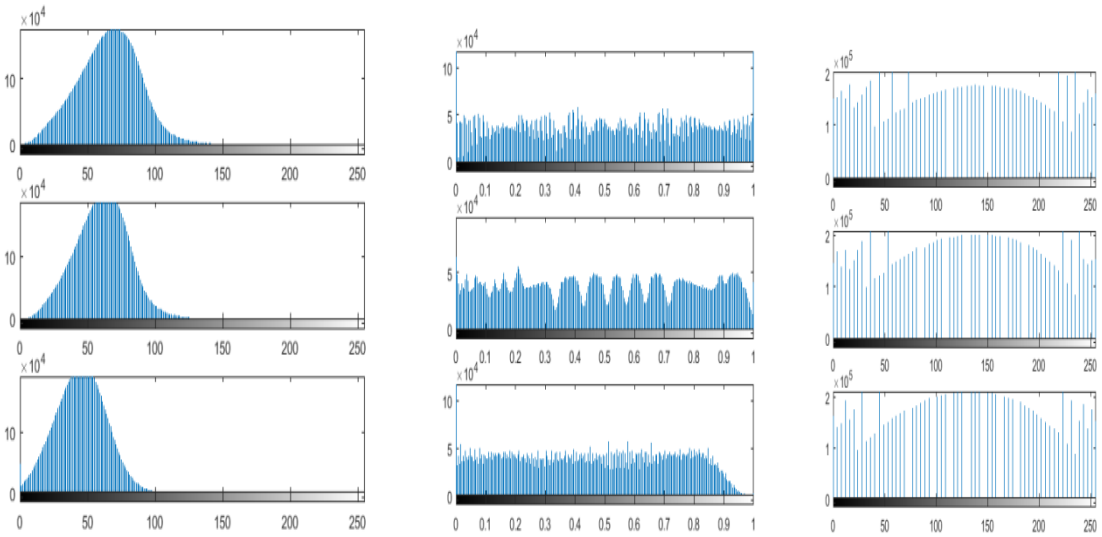

(a) (b) (c)

ISSN: 0975-8585

Figure-2: (colour online) Histogram-based RGB concentration of Figure 2. 2(a): RGB concentration of Figure 2(a), 2(b): RGB concentration of Figure 2(b), 2(c); RGB concentration of Figure 2(c)

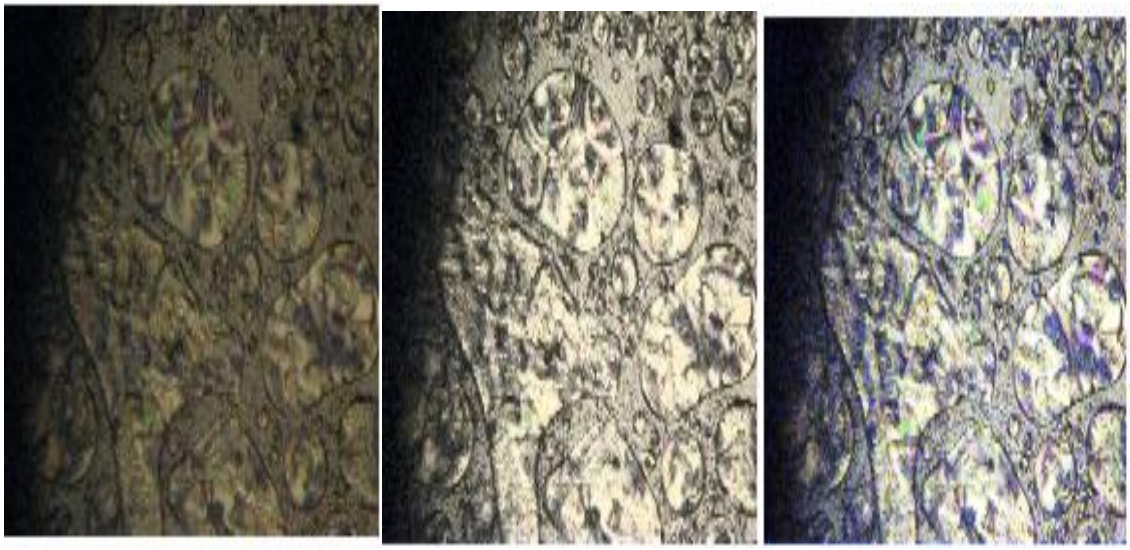

(a) (b) (c)

Figure-3: (colour online) Nematic phase 129 °C Nematic phase at 129 °C (2272 × 1704 pixels), (a) nematic texture, (b) true RGB colour image of original texture (a), (c) histogram equalized image with contrast enhancement

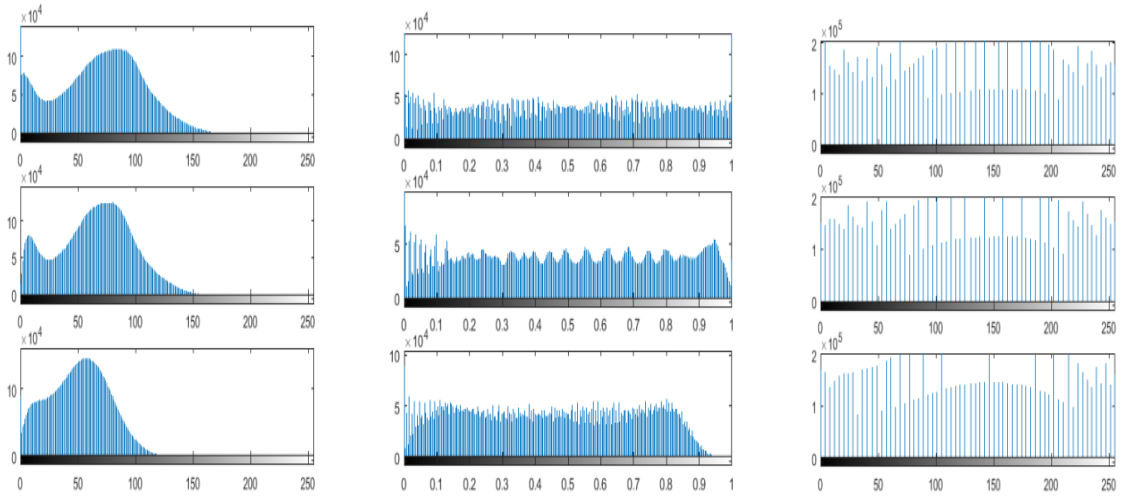

(a) (b) (c)

Figure-4: (colour online) Histogram-based RGB concentration of Figure 4. 4 (a): RGB concentration of Figure 4(a), 4(b): RGB concentration of Figure 4(b), 4(c); RGB concentration of Figure 4(c)

ISSN: 0975-8585

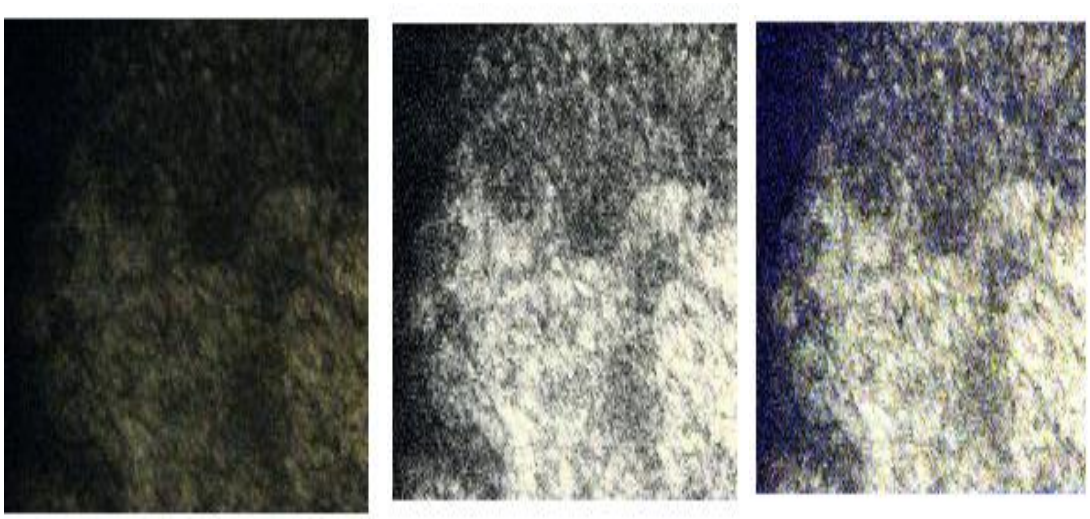

(a) (b) (c)

Figure-5: (colour online) smectic-c to solid I transition at 91 °C (2272 × 1704 pixels), (a) nematic texture, (b) true RGB colour image of original texture (a), (c) histogram equalized image with contrast enhancement

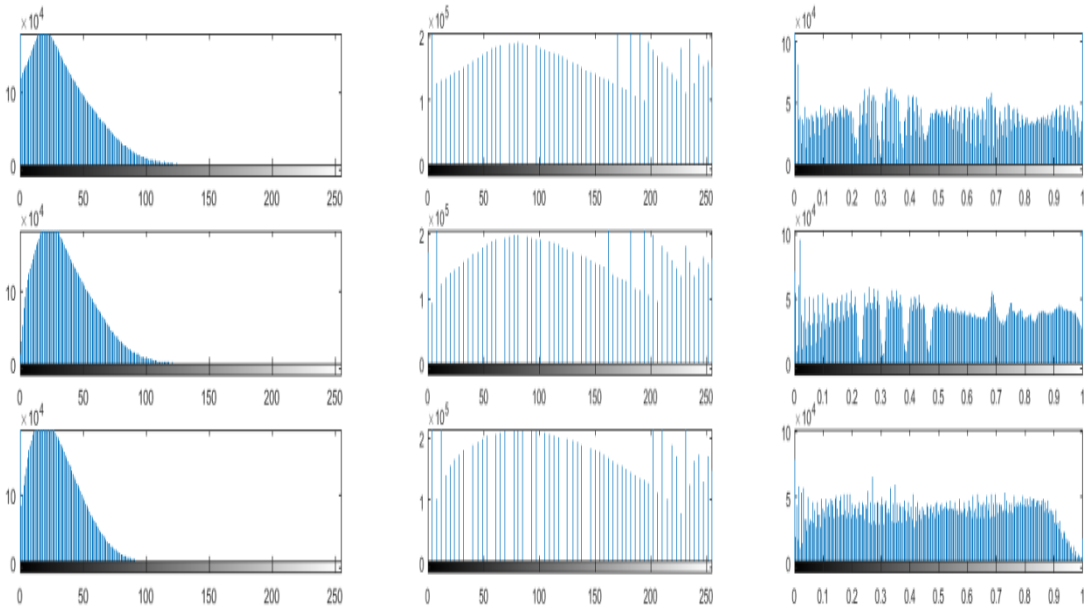

(a) (b) (c)

Figure-6: (colour online) Histogram-based RGB concentration of Figure 6. 6 (a): RGB concentration of Figure 6(a), 6(b): RGB concentration of Figure 6(b), 6(c); RGB concentration of Figure 6(c)

9OBA + 1 wt % of Fe_3O_4 nanoparticles:

ISSN: 0975-8585

(a) (b) (c)

Figure-7: (colour online) isotropic – nematic droplets at 131.4 °C (2272 × 1704 pixels), (a) nematic droplet texture, (b) true RGB colour image of original texture (a), (c) histogram equalized image with contrast enhancement

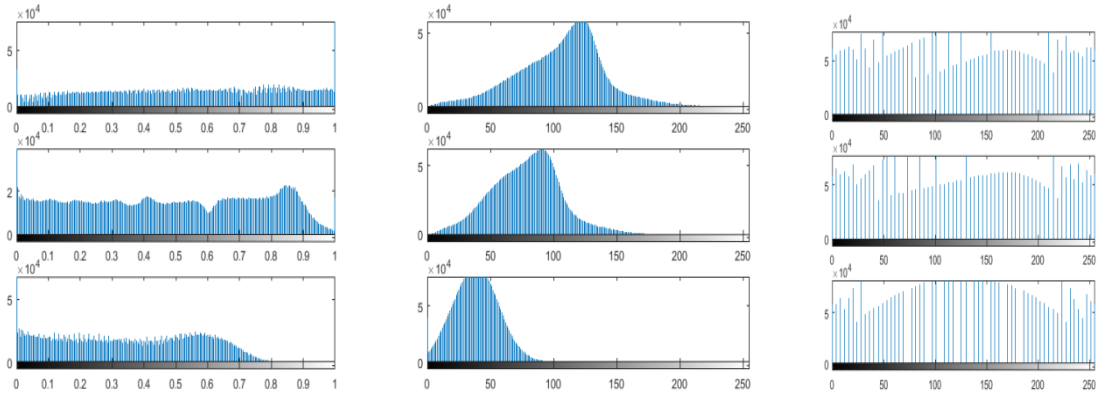

(a) (b) (c)

Figure-8: (colour online) Histogram-based RGB concentration of Figure 8. 8 (a): RGB concentration of Figure 8(a), 8(b): RGB concentration of Figure 8(b), 8(c); RGB concentration of Figure 8(c)

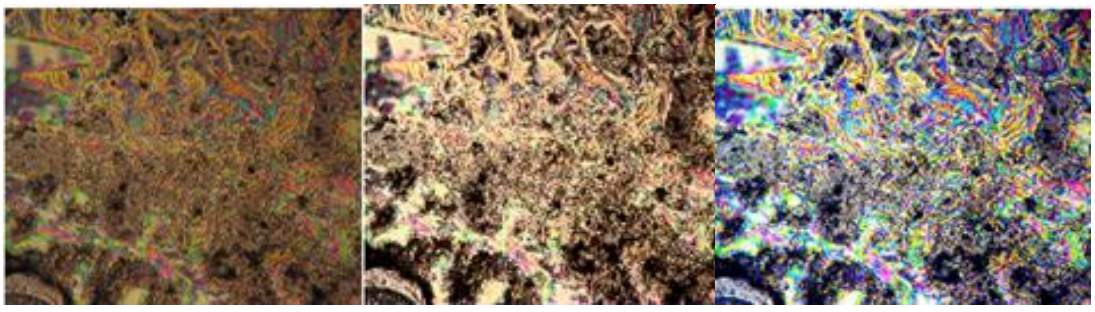

(a) (b) (c)

Figure-9: (colour online) nematic- smectic c transition at 108.3 °C (2272 × 1704 pixels), (a) nematic- smectic c texture, (b) true RGB colour image of original texture (a), (c) histogram equalized image with contrast enhancement

ISSN: 0975-8585

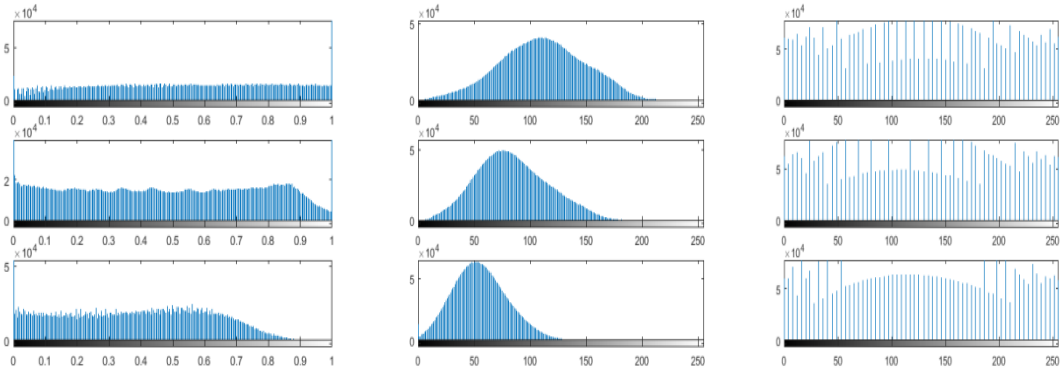

(a) (b) (c)

Figure-10: (colour online) Histogram-based RGB concentration of Figure 10. 10 (a): RGB concentration of Figure 10(a), 10(b): RGB concentration of Figure 10(b), 10(c); RGB concentration of Figure 10(c)

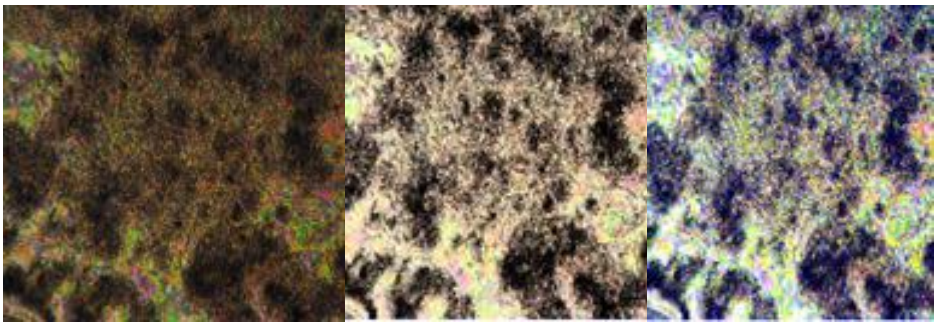

(a) (b) (c)

Figure-11: (colour online) sanded texture of smectic c texture at 103.5 °C (2272 × 1704 pixels), (a) sanded smectic c texture, (b) true RGB colour image of original texture (a), (c) histogram equalized image with contrast enhancement

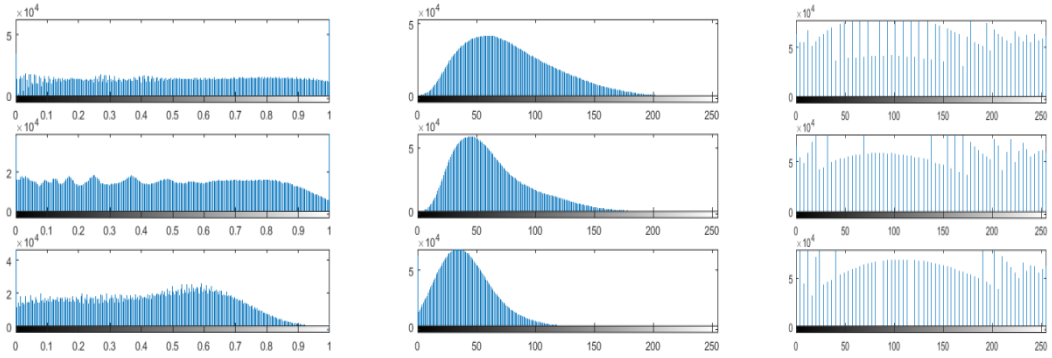

a) (b) (c)

Figure-12: (colour online) Histogram-based RGB concentration of Figure 12. 12 (a): RGB concentration of Figure 12(a), 12(b): RGB concentration of Figure 12(b), 12(c); RGB concentration of Figure 12(c)

ISSN: 0975-8585

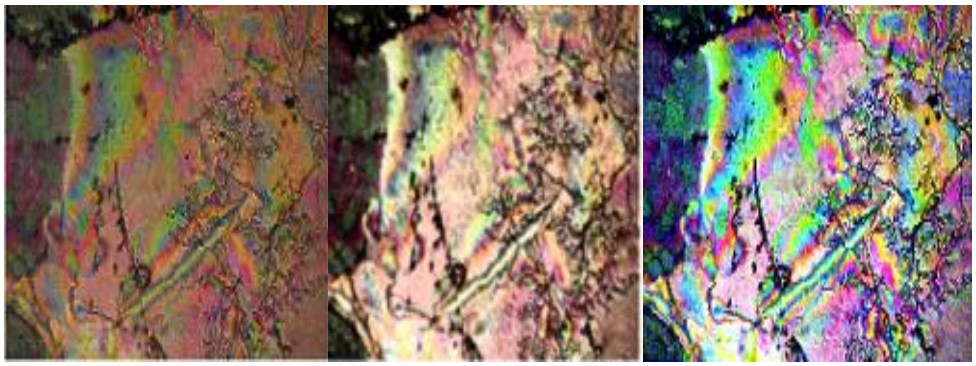

(a) (b) (c)

Figure-13: (colour online) solid I texture at 82 °C (2272 × 1704 pixels), (a) solid I texture, (b) true RGB colour image of original texture (a), (c) histogram equalized image with contrast enhancement

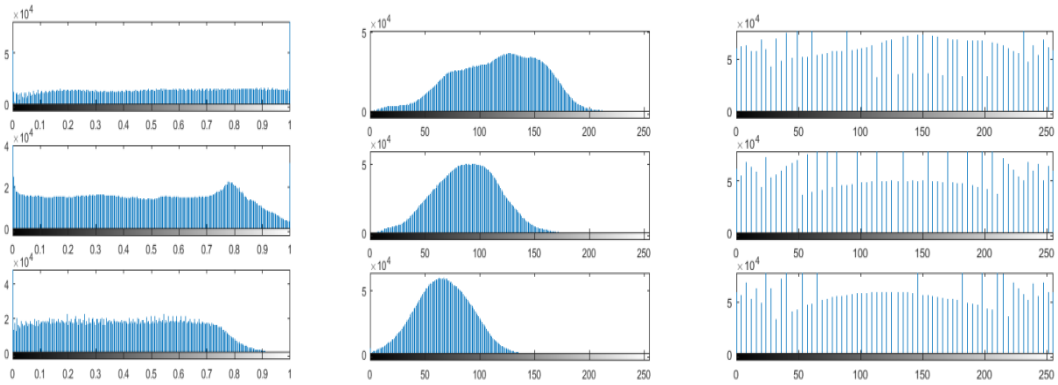

(a) (b) (c)

Figure-14: (colour online) Histogram-based RGB concentration of Figure 14. 14 (a): RGB concentration of Figure 14(a), 14(b): RGB concentration of Figure 14(b), 14(c); RGB concentration of Figure 14(c)

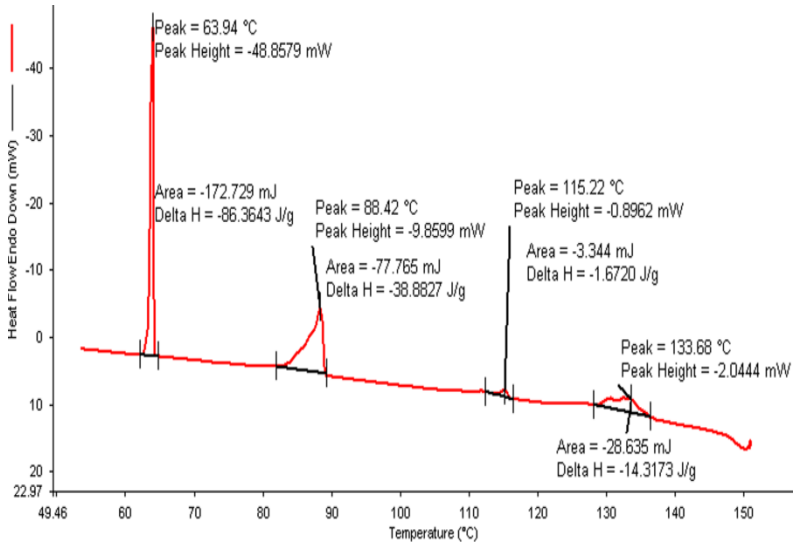

Figure-15: DSC curve of 9OBA pure compound (scan rate 20 °C/min)

ISSN: 0975-8585

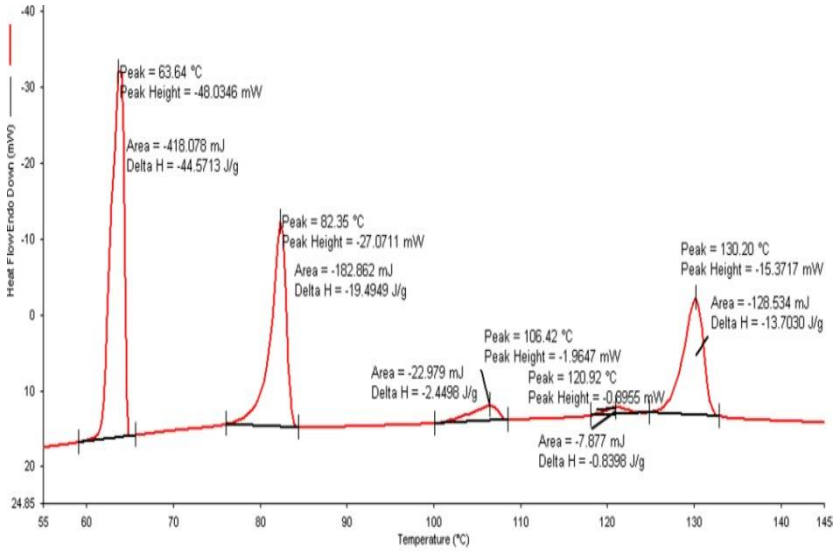

Figure-16: DSC curve of 9OBA + 1 wt % Fe_3O_4 nanoparticles (scan rate 20 °C/min)

Figure-2 shows histogram based RGB (Red, Green, and Blue) concentration. From Figure-2(a) we observed that histogram is concentrated towards darker side i.e. the intensity is focused towards left side of the graph. Figure-2(b) shows the low contrast RGB image of Figure-2(b), which is obtained by NTSC to RGB conversion. This is conformed as low contrast image from the evident that histogram is concentrated at middle portion in the Figure-2(b). From Figure-2(c) there is an improvement in average intensity and contrast are observed. The increase contrast is due to the considerable spread of the histogram over the entire intensity scale. The increase in overall intensity is due to the fact that the average intensity level in the histogram of the equalized image is higher than the original. The contrast of the image is enhanced at it is very easy to observe the defects in the texture. From the obtained images in this methodology, the black colored areas represent the local mean intensity, different from the total mean intensity of the image. This procedure is repeated at different transition temperatures of the 9OBA pure compound and 9OBA + 1 wt % Fe_3O_4 nanoparticles dispersion. The corresponding RGB concentration for original image, True RGB color image and histogram equalized image is presented from Figure-(3, 4) to Figure-(13, 14).
Further, from the results it is envisaged that

* The transition temperatures are reduced compared to the pure compound 9OBA as expected in nanoparticles dispersed 9OBA.
* The nematic range is increased by the dispersion of Fe_3O_4 nanoparticles in 9OBA as compared. Previously this procedure is adopted by Sastry et al. in the case of other liquid crystals [22, 23] and Madav et al. [24]. The DSC thermogram of 9OBA and with dispersion of Fe_3O_4 nanoparticles is given in Figure 15 & Figure 16 for comparison of the transition temperatures. They are in good agreement with the POM data and slight variation in the temperatures is due to the environmental variance (Table-1).

Table 1: Phase variants, transition temperatures, Enthalpy values of 9OBA pure and with dispersed 1 wt % of Fe_3O_4 nanoparticles

S. No	Compound	DSC/ POM	Transition temperatures ^oC				Thermal Ranges ^0C	
			I-N	N-SmC	SmC –Solid I	SolidI-Solid 2	ΔN	ΔSmC
1	9OBA Pure	DSC ΔHJ/g	133.68 14.317	115.22 1.672	88.42 38.88	63.94 86.364	18.48	26.8
		POM	134.9	116.0	91.0	63.0	18.9	25.0
2	9OBA + 1wt % Fe_3O_4	DSC ΔHJ/g	130.20 13.703	106.42 2.449	82.35 19.4949	63.64 44.571	23.78	24.07
		POM	131.4	108.3	83.5	64.2	23.1	24.8

CONCLUSION

In this paper the authors mainly discussed about the histogram equalization technique, performed on the pure 9OBA and 9OBA + 1 wt % of Fe_3O_4 nanoparticles dispersion to identify the defects in the textures by enhancing contrasts in the image. By increasing the visual appearance of the low contrast image with this current technique, the accurate identification of phases at transition temperatures are possible with naked eye. The obtained results of histogram equalization is giving the high contrast image which covers a broad range of the gray scale and further, the distribution of pixels is not too far from uniform, with very few vertical lines being much higher than the others. Further, the transition temperatures obtained from polarizing microscope attached with the hot stage are in good agreement with those obtained from DSC. The slight differences can be attributed due to the environmental variance.

ACKNOWLEDGEMENTS

The author Dr R.K.N.R. Manepalli (Dr M. Ramakrishna Nanchara Rao) is thankful to the UGC for grant 42-784/2013 (SR).

REFERENCES

[1] Gonzalez RC, Woods RE. Digital Image Processing 2002; Prentice Hall: 2nd edition.
[2] Pei SC, Zeng YC, Chang CH. IEEE Trans Image Proc 2004; 13: 416-429.
[3] Wahad A, Chin SH, Tan EC. IEEE Proc 1998; 145: 160-166.
[4] Torre A, Peinado AM, Segura JC, Perez-Cordoba JL, Benitez MC, Rubio AJ. IEEE Trans Speech Audio Proc 2005; 13: 355-366.
[5] Pizer SM. IEEE Trans Med Image 2003; 22: 2-10.
[6] Lau S. Elect Lett 1994; 30: 122–123.
[7] Kim YT. IEEE Trans Cons Elect 1997; 43: 1-8.
[8] Kim TK, Paik JK, Kang BS. IEEE Trans Cons Elect 1998; 44: 82-87.
[9] Wang Y, Chen Q, Zhang B. IEEE Trans Cons Elect 1999; 45: 68-75.
[10] Chen SD, Ramli AR. IEEE Trans Cons Elect 2003; 49: 1301-1309.
[11] Wang Q, Ward RK. IEEE Trans Cons Elect 2007; 53: 757-764.
[12] Yoon H, Han Y, Hahn H, Image contrast enhancement based sub histogram equalization technique without over-equalized noise, International conference on control, automation and system engineering 2009; 176-182.
[13] Buzuloiu V, Ciuc M, Rangayyan R.M, Vertan C. J Elect Imaging 2001; 10: 445-459.
[14] Chanda B, Majumder DD. Digital Image Processing and Analysis 2002; Prentice-Hall
[15] Rao MC. Optoelect & Adv Mater (Rapid Commu) 2011; 5: 85-88.
[16] Muntaz Begum Sk, Rao MC, Ravikumar RVSSN. Spectrochim Acta Part A Mol & Biomol Spec 2012; **98**: 100-104.
[17] Muntaz Begum Sk, Rao MC, Ravikumar RVSSN. J Inorg Organometa Poly Mater 2013; 23(2): 350-356.
[18] Rao MC. J Optoelect & Adv Mater 2011; 13: 428-431.
[19] Rao MC, Hussain OM. Eur Phys J Appl Phys 2009; 48(2): 20503
[20] Rao MC. Optoelect & Adv Mater (Rapid Commu) 2011; 5(5-6): 651-654.
[21] Gray GW. Molecular structures and properties of liquid crystals 1962; Academic press, Newyork.
[22] Sreehari Sastry S, Mallika K, Gowri Sankara Rao B, Tiong HS, Lakshminarayana S. Liquid Crystals 2012; 39: 1–4.
[23] Sreehari Sastry S, Mallika K, Vishwam T, Lakshminarayana S, Tiong HS. Liquid Crystals 2014; 41: 558-571.
[24] Madhav BTP, Pardhasaradhi P, Manepalli RKNR, Pisipati VGKM. Liquid Crystals 2015; 1-9.